Antiviral Research 141 (2017) 101–106

Contents lists available at ScienceDirect

Antiviral Research

journal homepage: www.elsevier.com/locate/antiviral

Identification and evaluation of potent Middle East respiratory syndrome coronavirus (MERS-CoV) 3CL^{Pro} inhibitors

Vathan Kumar [a, 1], Jin Soo Shin [b, 1], Jiun-Jie Shie [c], Keun Bon Ku [b], Chonsaeng Kim [b], Yun Young Go [b], Kai-Fa Huang [a], Meehyein Kim [b, **], Po-Huang Liang [a, d, *]

[a] Institute of Biological Chemistry, Academia Sinica, Taipei, Taiwan
[b] Korea Research Institute of Chemical Technology, Daejeon, Republic of Korea
[c] Institute of Chemistry, Academia Sinica, Taipei, Taiwan
[d] Institute of Biochemical Sciences, National Taiwan University, Taipei, Taiwan

ARTICLE INFO

Article history:
Received 13 September 2016
Received in revised form
10 February 2017
Accepted 14 February 2017
Available online 17 February 2017

Keywords:
MERS-CoV
SARS-CoV
3C-like protease
Peptidomimetic inhibitor
Coronavirus
Picornavirus

ABSTRACT

Middle East respiratory syndrome coronavirus (MERS-CoV) causes severe acute respiratory illness with fever, cough and shortness of breath. Up to date, it has resulted in 1826 human infections, including 649 deaths. Analogous to picornavirus 3C protease (3C^{pro}), 3C-like protease (3CL^{pro}) is critical for initiation of the MERS-CoV replication cycle and is thus regarded as a validated drug target. As presented here, our peptidomimetic inhibitors of enterovirus 3C^{pro} (**6b**, **6c** and **6d**) inhibited 3CL^{pro} of MERS-CoV and severe acute respiratory syndrome coronavirus (SARS-CoV) with IC_{50} values ranging from 1.7 to 4.7 μM and from 0.2 to 0.7 μM, respectively. In MERS-CoV-infected cells, the inhibitors showed antiviral activity with EC_{50} values ranging from 0.6 to 1.4 μM, by downregulating the viral protein production in cells as well as reducing secretion of infectious viral particles into culture supernatants. They also suppressed other α- and β-CoVs from human and feline origin. These compounds exhibited good selectivity index (over 70 against MERS-CoV) and could lead to the development of broad-spectrum antiviral drugs against emerging CoVs and picornaviruses.

1. Introduction

Coronaviruses (CoVs) affecting upper respiratory tract were first identified in humans in mid-1960 (Tyrrell and Bynoe, 1965). In late 2002, there was emergence of a life threatening CoV of atypical pneumonia, named severe acute respiratory syndrome CoV (SARS-CoV). SARS-CoV belongs to the family *Coronaviridae*, and is an enveloped, positive-stranded RNA virus with ~30,000 nucleotides (Rota et al., 2003). Its genome encodes two polyproteins, pp1a (~490 kDa) and pp1ab (~790 kDa) which are processed by 3C-like protease (3CL^{pro}) and papain-like protease (PL^{pro}) to generate non-structural proteins essential for viral replication (Thiel et al., 2001, 2003). Due to its vital role in replication, 3CL^{pro} has been regarded as a validated drug target. Many inhibitors of SARS-CoV 3CL^{pro} were discovered by high throughput screening and structure-based rational design as summarized in the review articles (Hilgenfeld and Peiris, 2013; Kumar et al., 2013; Kuo and Liang, 2015; Pillaiyar et al., 2016; Ramajayam et al., 2011; Tong, 2009; Zhao et al., 2013). After SARS-CoV infection subsided, Middle East respiratory syndrome CoV (MERS-CoV), has emerged in Saudi Arabia in 2012 and spread worldwide, killing 36% of the reported 1826 patients (http://www.who.int/mediacentre/factsheets/mers-cov/en/). Due to the similar maturation pathway, MERS-CoV 3CL^{pro} is also regarded as a target for developing antiviral drugs (Tomar et al., 2015). Though tremendous efforts have been made to develop inhibitors, therapeutic interventions for such continuous CoV outbreaks are yet to reach market (Barnard and Kumaki, 2011; Kilianski and Baker, 2014).

These CoVs' 3CL^{pro} are functionally similar to the 3C^{pro} in picornaviruses and both adopt chymotrypsin fold (Anand et al., 2003). However, 3CL^{pro} is a dimer with Cys-His dyad, whereas 3C^{pro} is a monomer with Cys-His-Glu triad (Hsu et al., 2005; Lee

* Corresponding author. Institute of Biological Chemistry, Academia Sinica, Taipei 115, Taiwan.
** Corresponding author. Center for Virus Research and Testing, Korea Research Institute of Chemical Technology, 141 Gajeongro, Yuseong, Daejeon 34114, Republic of Korea.
E-mail addresses: mkim@krict.re.kr (M. Kim), phliang@gate.sinica.edu.tw (P.-H. Liang).
[1] These authors contributed equally to this work.

http://dx.doi.org/10.1016/j.antiviral.2017.02.007
0166-3542/

et al., 2009; Yang et al., 2003). Picornaviruses are small, non-enveloped RNA virus with genome size of 7500–8000 nucleotides. Based on their genetic organization, the family is composed of 31 genera including *Enterovirus* (enterovirus and rhinovirus), *Aphthovirus* (foot-and-mouth disease virus), *Cardiovirus* (encephalomyocarditis virus), *Hepatovirus* (hepatitis A virus) and others (http://www.picornaviridae.com/). As $3C^{pro}$ is produced in all genera of *Picornaviridae* virus family, its inhibitors showed broad-spectrum, potent antiviral activity against rhinovirus, coxsackievirus and enterovirus (Jetsadawisut et al., 2016; Kim et al., 2015; St John et al., 2015). Though $3C^{pro}$ and $3CL^{pro}$ share similar structures at their active sites, subtle differences often discriminate inhibitors. AG7088, an established $3C^{pro}$ inhibitor, was inactive against SARS-CoV $3CL^{pro}$ prior to the modifications (Ghosh et al., 2005; Shie et al., 2005; Thanigaimalai et al., 2013; Yang et al., 2006). Unlike AG7088 which contains α, β-unsaturated ester for forming covalent bond with the active-site Cys, our previously reported potent peptidomimetic inhibitors of $3C^{pro}$ from enterovirus 71 (EV71) contains aldehyde as electrophilic warhead (Kuo et al., 2008). In this work, we screened those EV71 $3C^{pro}$ inhibitors against MERS-CoV $3CL^{pro}$ and further evaluated the hits by cell-based assays using live MERS-CoV. Our best compounds **6b**, **6c** and **6d** inhibited MERS-CoV $3CL^{pro}$ with IC_{50} values ranging from 1.7 to 4.7 μM and also suppressed viral replication with EC_{50} values between 0.6 and 1.4 μM. These derivatives represent some of few cell-based assay-confirmed anti-MERS-CoV agents and also showed broad-spectrum activity against both α- and β-types of CoVs as described herein.

2. Materials and methods

2.1. Synthesis of compounds

Compounds reported here were synthesized using previously reported procedures with some modifications (Kuo et al., 2008). Test compounds and gemcitabine hydrochloride (GEM; Sigma-Aldrich, St. Louis, MO) were dissolved in dimethyl sulfoxide (DMSO; Sigma-Aldrich) at 50 μM concentration.

2.2. Viruses and cells

Patient-derived isolate MERS-CoV (MERS-CoV/KOR/KNIH/002_05_2015; GenBank accession No. KT029139) was provided by the Korea Center for Disease Control and Prevention. Huh-7 and Vero cells (Cat. No. CCL-81) were obtained from Prof. D.-E. Kim at Konkuk University (Seoul, Republic of Korea) and American Type Culture Collection (ATCC, Manassas, VA), respectively. The cells were maintained in Dulbecco's Modified Eagle Medium (DMEM; Gibco BRL, Grand Island, NY) supplemented with 10% fetal bovine serum (FBS; Gibco BRL) at 37 °C and 5% CO_2. To minimize adaptive mutation probability of MERS-CoV to another species during passage, MERS-CoV was amplified by infection of a human cell line, Huh-7 cells. The infectious viral titers from culture supernatants at day 2 post-infection (p.i.) were measured by a plaque assay using Vero cells according to other reports (Chan et al., 2013; de Wilde et al., 2013). MERS-CoV was maintained under biosafety level 3 conditions in Korea Research Institute of Chemical Technology (KRICT).

Human CoV strains, 229E (Cat. No. VR-740) and OC43 (Cat. No. VR-1558) were purchased from ATCC. They were amplified by infecting human fetal lung fibroblast MRC-5 cells (ATCC, Cat. No. CCL-171). Feline infectious peritonitis coronavirus (FIPV) strain (Cat. No. VR-990) and its host cell line Crandall feline kidney (CRFK) (Cat. No. 10094) were obtained from ATCC and Korean Cell Line Bank (Seoul, Republic of Korea), respectively.

2.3. Expression and purification of SARS- and MERS-CoV $3CL^{pro}$

The expression and purification of SARS-CoV $3CL^{pro}$ followed our reported procedure (Kuo et al., 2004). For expression of MERS-CoV $3CL^{pro}$ (Kumar et al., 2016), the Factor Xa cleavage site (IEGR) and the $3CL^{pro}$ (accession KJ361502.1, Ser3248–Gln3553) DNA sequence was synthesized and cloned into the pET32 expression vector by Mission Biotech. Company (Taiwan) and was transformed into *E. coli* BL21 (DE3). A 10 ml overnight culture of a single transformant was used to inoculate 1L of fresh LB medium containing 100 μg/ml ampicillin. The cells were grown at 37 °C to $A_{600} = 0.8$ and induced with 0.4 mM isopropyl-β-thiogalactopyranoside (IPTG) for 22 h at 16 °C. The cells were harvested by centrifugation at 7000 × *g* for 15 min and the pellet was suspended in lysis buffer (12 mM Tris-HCl, 120 mM NaCl, 0.1 mM EDTA, and 5 mM DTT, pH 7.5). A French-press instrument (Constant Cell Disruption System) was used to disrupt the cells at 20,000 psi and centrifuged at 20,000 × *g* for 1 h to discard the debris. The cell-free extract was loaded onto Ni-NTA column which was equilibrated with lysis buffer containing 5 mM imidazole. After exhaustive washing with lysis buffer, the imidazole concentration of the washing buffer was increased to 30 mM. The protein eluted by lysis buffer containing 300 mM imidazole was dialyzed against lysis buffer to remove imidazole and then Factor Xa was added to a final concentration of 1% (w/w) and incubated at 16 °C for 24 h to remove the His-tag. Subsequently, the processed MERS-CoV $3CL^{pro}$ was passed through a Ni-NTA column for purification. The protein concentration was determined by the protein assay kit (BioRad, USA) and BSA was used as standard.

2.4. Measurement of IC_{50}

A fluorometric assay by using the fluorogenic peptide, Dabcyl-KTSAVLQSGFRKME-Edans as previously described (Kuo et al., 2004) was used to determine the inhibition constants of compounds. The enhanced fluorescence due to the cleavage of this substrate catalyzed by the $3CL^{pro}$ was monitored at 538 nm with excitation at 355 nm. The IC_{50} value of individual sample was measured in a reaction mixture containing 50 nM SARS-CoV $3CL^{pro}$ or 0.3 μM MERS-CoV $3CL^{pro}$ and 10 μM of the fluorogenic substrate in 20 mM Bis-Tris (pH 7.0).

2.5. Cytopathic effect inhibition assay

Huh-7 cells were seeded in 96-well plates (2×10^4 cells per well). On the next day, cells were infected with MERS-CoV at a multiplicity of infection (MOI) of 0.1 in DMEM without FBS for 1 h. After washing with PBS, mock-infected or virus-infected cells were treated with 3-fold serial dilutions of test compounds or GEM used as a positive control. At day 2 p.i., cell lysate was harvested for measuring cell viability using the CellTiter 96® AQ_{ueous} One Solution Cell Proliferation Assay according to the manufacturer's instructions (Promega, Madison, WI). The 50% cytotoxic concentration (CC_{50}) and 50% effective concentration (EC_{50}) values were calculated using GraphPad Prism 6 software (GraphPad Software, La Jolla, CA). Antiviral assay for other CoVs, including 229E, OC43 and FIPV strains, were performed as mentioned above by using different cell lines. MRC-5 cells were used for culturing human CoVs, 229E and OC43, while CRFK cells for feline CoV, FIPV.

2.6. Western blot analysis

Huh-7 cells seeded in 6-well plates (3×10^5 cells per well) were infected with MERS-CoV at an MOI of 0.02 for 1 h. After washing with PBS, cells were treated with 0.1, 1 and 10 μM of compounds **6b**,

Table 1
Enzymatic and cell-based antiviral assays of selected compounds.

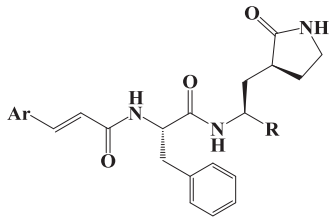

Compd	Ar	R	IC_{50} (μM)		CC_{50} (μM)[a]	EC_{50} (μM) MERS-CoV	S.I.[b]
			MERS-CoV $3CL^{pro}$	SARS −CoV $3CL^{pro}$			
4a	3,4-$(OCH_2O)C_6H_3$	$-COOCH_3$	>25	>25	ND[c]	ND	ND
5a	3,4-$(OCH_2O)C_6H_3$	$-CH_2OH$	>25	>25	ND	ND	ND
6a	3,4-$(OCH_2O)C_6H_3$	−CHO	>25	>25	>100	>100	ND
6b	3-BrC_6H_4	−CHO	2.4 ± 0.3	0.7 ± 0.2	>100	1.4 ± 0.0	>71.4
6c	4-$Me_2NC_6H_4$	−CHO	4.7 ± 0.6	0.5 ± 0.1	>100	1.2 ± 0.6	>83.3
6d	4-Cl,2-FC_6H_3	−CHO	1.7 ± 0.3	0.2 ± 0.07	58.6 ± 1.2	0.6 ± 0.0	97.9
GEM[d]	–	–	ND	ND	>100	8.3 ± 0.9	>12.1

[a] 50% cytotoxic concentration in MDCK cells.
[b] Selectivity index.
[c] Not determined.
[d] Gemcitabine hydrochloride.

6c and **6d**. In parallel, 0.02% DMSO was treated as a compound vehicle. On day 1 p.i., 30 μg cell lysates suspended in sample loading buffer (Biosesang, Gyeonggi-do, Republic of Korea) were subjected to 10% SDS-PAGE and electro-transferred to a polyvinylidene fluoride membrane (Millipore, Billerica, MA). MERS-CoV NP was detected using a primary antibody specific for viral nucleocapsid protein (NP) (Cat. 100211-RP02; Sino Biological Inc., Beijing, China), followed by a horseradish peroxidase (HRP)-conjugated goat anti-rabbit secondary antibody (Thermo Scientific, Waltham, MA). The cellular β-actin protein, a loading control, was detected with an anti-β-actin-specific primary antibody (Cat. No. A1987; Sigma-Aldrich) and the HRP-conjugated goat anti-mouse secondary antibody (Thermo Scientific). After addition of a chemiluminescent HRP substrate (SuperSignal West Pico Chemiluminescent Substrate; Pierce, Rockford, IL), images were obtained using a LAS-4000 Luminescent Image Analyzer (Fujifilm, Tokyo, Japan).

2.7. Plaque inhibition assay

Huh-7 cells were inoculated in 6-well plates at a density of 1×10^6 cells per well for 1 day. Culture supernatants treated with 1 μM compounds were harvested at day 1 p.i. They were serially diluted 10-fold in DMEM from 10^{-1} to 10^{-3} and 1 ml of each sample was used to infect Vero cells for 1 h. After washing with PBS to remove unabsorbed virus, DMEM containing 0.5% agarose (overlay medium) was added. On day 3 p.i., plaques were visualized with 50 μg/ml neutral red (Sigma-Aldrich).

3. Results and discussion

3.1. Inhibition of MERS-CoV $3CL^{pro}$ and viral infection by **6b**, **6c** and **6d**

Peptidomimetic compounds were synthesized according to our reported method (Kuo et al., 2008). Preliminary screening of these peptidomimetic compounds against MERS $3CL^{pro}$ were done at 50 μM. Compounds inhibiting more than half of the protease activity under such condition were selected for further IC_{50} measurements. Using enzymatic assay, the compounds **6b**, **6c** and **6d** showed IC_{50} of 2.4, 4.7 and 1.7 μM against purified $3CL^{pro}$ of MERS-CoV, respectively (Table 1). These compounds also inhibited SARS $3CL^{pro}$ at lower IC_{50} values of 0.7, 0.5 and 0.2 μM, respectively.

To evaluate the ability of these compounds to block viral replication, we performed cytopathic inhibition assay using MERS-CoV-infected Huh-7 cells. As shown in Fig. 1, compounds **6b**, **6c** and **6d** efficiently suppressed viral replication with EC_{50} of 1.4, 1.2 and 0.6 μM, respectively (Table 1). Though it is usual to see EC_{50} higher than IC_{50}, due to the presence of membrane barrier, we observed EC_{50} to be smaller than IC_{50}. This could be due to the higher concentration (300 nM) used for *in-vitro* enzymatic assay because it is a weakly associated dimer (Tomar et al., 2015). In fact, they inhibited 50 nM SARS $3CL^{pro}$, a tight dimer, in the submicromolar range (Table 1). These compounds had CC_{50} larger than 100 μM for **6b** and **6c** or 58.6 μM for **6d** against uninfected cells, resulting in selectivity index (S.I.) values larger than 71.4. As expected, compound **6a** which was inactive in the enzyme assay did not suppress viral replication. GEM, used as a positive control according to a previous report (Dyall et al., 2014), was less potent in inhibiting MERS-CoV infection with an EC_{50} value of 8.3 μM. It also showed marginal toxicity and thus decreased viability of mock cells by 20% or more at the concentrations above 3.7 μM (Table 1 and Fig. 1).

3.2. Suppression of viral protein production and infectious MERS-CoV generation

To confirm that the observed antiviral activity of compounds **6b**, **6c** and **6d** reflects inhibition of MERS-CoV infection, both viral protein and progeny production was measured after treatment of virus-infected cells with these compounds. Western blot analysis showed that viral NP was decreased by these inhibitors in a dose-dependent manner (Fig. 2). It is noteworthy that no viral NP detectable in the presence of 10 μM $3CL^{pro}$ inhibitors.

We further compared the number of infectious MERS-CoV particles in the culture supernatants, both in the presence and absence of $3CL^{pro}$ inhibitors. The plaque assay showed that the viral titer in the absence of compound was 4.4×10^5 plaque forming units (pfu)/ml, but reduced to 1.7×10^4, 2.9×10^4, and 1.2×10^4 pfu/ml by 1 μM of compounds **6b**, **6c** and **6d**, respectively (Fig. 3). Taken together,

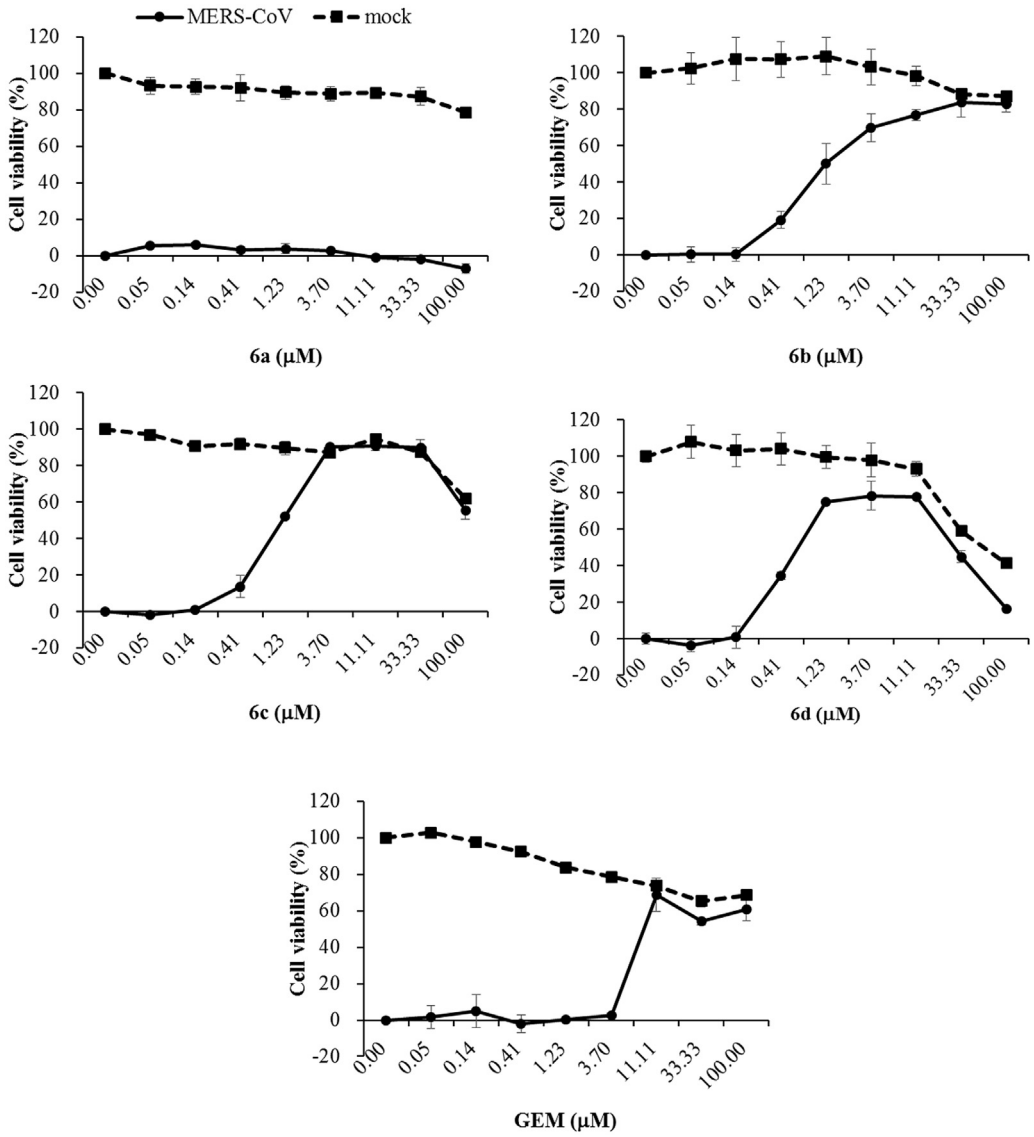

Fig. 1. Antiviral activity of 6b, 6c and 6d against MERS-CoV in Huh-7 cells. Huh-7 cells in 96-well plates were mock-infected or infected with MERS-CoV at an MOI of 0.1 for 1 h at 37 °C. After washing with PBS, cells were treated with 3-fold serial dilutions of test compounds (**6a**, **6b**, **6c** and **6d**) or a control compound (GEM). On day 2 p.i., cell lysates were harvested for measuring cell viability. The data represent the means ± standard deviations from three independent experiments.

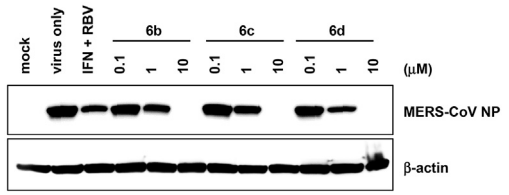

Fig. 2. Inhibition of MERS-CoV NP production by 6b, 6c and 6d in a dose-dependent manner. Huh-7 cells in 6-well plates were infected with MERS-CoV at an MOI of 0.02 for 1 h at 37 °C.The virus-infected cells were treated with increasing concentrations (0.1, 1 and 10 μM) of each compound. Co-treatment of interferon-alpha 2A (IFN; 50 ng/ml) and ribavirin (RBV; 100 μM) was used as a positive control. On day 1 p.i., cells were harvested and loaded to 10% SDS-PAGE (30 μg per well). Immunoblotting was performed using rabbit anti-NP antibody and HRP-conjugated goat anti-rabbit secondary antibody. β-Actin was used as a loading control.

the results suggest that the compounds originally selected as EV71 $3C^{pro}$ blockers efficiently inhibited MERS-CoV $3CL^{pro}$ activity and suppressed viral protein production as well as viral progeny generation. The data also indicate that the inhibitors can penetrate virus-infected cell membrane to reach the active site of $3CL^{pro}$.

3.3. *In silico molecular docking of **6d** against MERS-CoV $3CL^{pro}$*

To rationalize potent inhibition, we docked **6d** into the active site of MERS-CoV $3CL^{pro}$. The initial pose of the complex was generated based on the X-ray structure (PDB code: 4RSP) of the $3CL^{pro}$ in complex with a covalent inhibitor (Tomar et al., 2015) and those of the human rhinovirus $3C^{pro}$ bound with irreversible inhibitors (Matthews et al., 1999; Webber et al., 1998). Then, the simulation was done by Discovery Studio (Accelrys Inc., San Diego, CA). A Cys at subsite S1 of $3CL^{pro}$ acts as a nucleophile to cleave substrates by attacking carbonyl carbon of the amide bond between the conserved Gln at P1 and the small amino acids such as Ser, Ala or Gly at P1' (Fan et al., 2004; Needle et al., 2015). Our modelling shows that the γ-sulfur of Cys148 forms a covalent bond with the **6d** aldehyde carbon and the resulting oxyanion is stabilized by His41 (Fig. 4). A cyclic lactam moiety with *cis*-amide geometry on

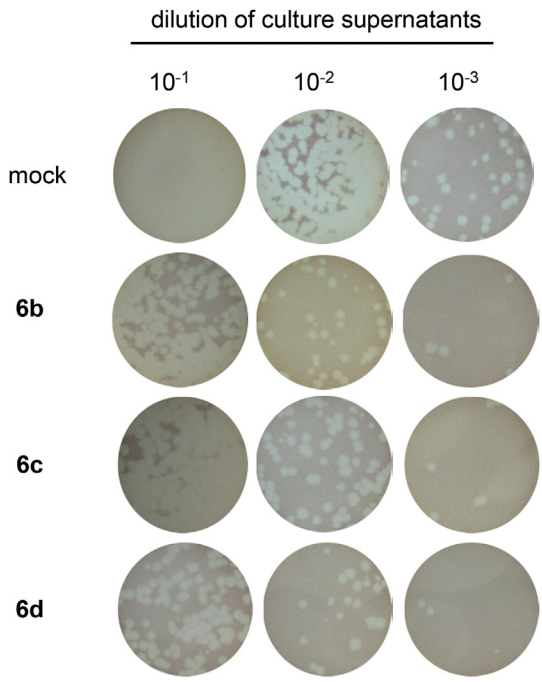

Fig. 3. Downregulation of MERS-CoV progeny generation by 3CL^{pro} inhibitors, 6b, 6c and 6d. MERS-CoV-infected Huh-7 cells in 6-well plates were treated with 1 μM **6b**, **6c** and **6d** for 1 day. Culture supernatants were harvested and serially diluted by 10-fold in DMEM (10^{-1} to 10^{-3}). Fresh Vero cells in 6-well plates were infected with the diluted cell culture inoculum for 1 h. And the number of infectious viral particles was counted by addition of the overlay medium for 3 days and by neutral red staining.

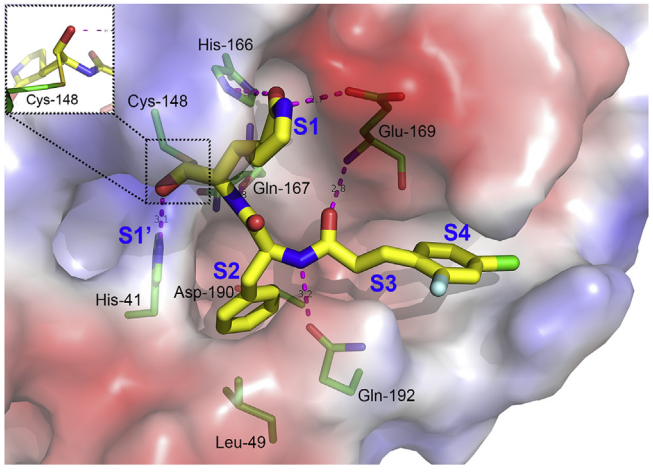

Fig. 4. Docking of inhibitor 6d with MERS-CoV 3CL^{pro}. Cys148 of the protease makes a covalent bond with the carbonyl carbon of the inhibitor aldehyde, forming a stable tetrahedral species (the inset), and the resulting oxyanion being stabilized by His 41. The protease is shown in a charge-potential surface. The putative substrate-binding subsites S1′, S1, S2, S3 and S4 are indicated. Moreover, the possible hydrogen bonds of **6d** to the protease are further drawn with dashed lines.

binding to 3C^{pro} was proposed to mimic the P1 Gln of peptide substrates (Matthews et al., 1999). Based on our docking results, the P1 lactam moiety of **6d** binds to S1 subsite of 3CL^{pro} by forming H-bonds with His166 and Glu169. The P2 phenylalanine moiety prefers to occupy S2 subsite. The cinnamoyl group of **6d** occupies S3 and may be extended to S4. The amide group between phenylalanine and cinnamoyl group further forms H-bonds with Gln192 and Glu169. We also docked **6d** based on the apo-form MERS-CoV 3CL^{pro} structure (PDB code: 5c3n) (Ho et al., 2015). Since the free-form and ligand-bound structures showed no significant difference in the active site, the binding modes of **6d** in these two structures are indeed very similar (data not shown).

Table 2
Antiviral activity of **6b**, **6c**, and **6d** against 229E, OC43 and FIP.

Compd	CC_{50}[a] (μM)	EC_{50} (μM) (S.I)		
		229E[b]	OC43[c]	FIPV[d]
6b	>100	4.3 ± 0.1 (>25.0)	13.5 ± 0.8 (>7.3)	2.5 ± 1.1 (>40.0)
6c	>100	4.2 ± 0.3 (>23.8)	16.8 ± 0.3 (>6.0)	1.9 ± 0.2 (>52.6)
6d	>100	2.0 ± 0.2 (>50.0)	17.7 ± 1.6 (>5.7)	1.1 ± 0.3 (>90.9)

[a] 50% cytotoxic concentration in MRC-5 cells and in CRFK cells.
[b] Human alpha coronavirus.
[c] Human beta coronavirus.
[d] Feline infectious peritonitis alpha coronavirus.

From our experimental as well as modelling results, substituents on cinnamoyl groups of these peptidomimetic inhibitors seem to be critical for the activity. Substituent *p*-chloro in **6d** makes halogen bonding with His194, leading to better potency. Compound **6b** and **6c** with slightly bulkier *m*-bromo and *p*-dimethylamino moiety, respectively, displayed approximately 2-fold drop in IC_{50}. Compound **6a** with the bulkiest 3,4-methylenedioxy substituent failed to inhibit the 3CL^{pro} even at 25 μM. Compounds **4a** and **5a** that lacked aldehyde warhead failed to inhibit 3CL^{pro}, emphasizing the importance of reactive aldehyde electrophile.

3.4. Broad spectrum activity against human and feline CoVs

To investigate for broad spectrum activity, three compounds were tested against human and feline CoVs. The result showed both α-CoVs, human 229E strain and FIPV, and β-CoV (human OC43 strain) were sensitive to the compounds with EC_{50} of 1.1–17.7 μM (Table 2), suggesting potent and broad-spectrum antiviral activities of these 3CL^{pro} inhibitors. The CC_{50} values measured using MRC-5 and CRFK cells, used to cultivate human and feline CoVs, respectively, were found to be more than 100 μM. Therefore, the S.I. values were ranged above 5.7 as shown in parentheses.

Peptide and peptidomimetic aldehyde inhibitors against 3CL^{pro} have been reported (Akaji et al., 2008, 2011; Zhu et al., 2011) but not tested on live CoVs. However, a potent SARS-CoV 3CL^{pro} peptidomimetic aldehyde inhibitor, TG-0205221, has been shown to block SARS-CoV and human CoV 229E replications (Yang et al., 2006). As shown in this study, we have identified potent and membrane-permeable MERS-CoV inhibitors **6b**, **6c** and **6d** using live MERS-CoV virus with EC_{50} of 0.6–1.2 μM and S.I. over 71.4. These compounds with $IC_{50} < 0.5$ μM against 3C^{pro} (Kuo et al., 2008) inhibited 3CL^{pro} of MERS-CoV with IC_{50} of 1.7–4.7 μM and SARS-CoV with IC_{50} of 0.2–0.7 μM. Moreover, we found these inhibitors were active against other viruses, including α- and β-CoVs with EC_{50} of 1.1–17.7 μM, but were less potent (higher EC_{50}) in killing human β-CoV OC43. Although not as potent as inhibiting picornavirus EV71 with the EC_{50} of 18 and 7 nM for **6c** and **6d**, respectively (Kuo et al., 2008), they are the most potent inhibitors of live MERS-CoV identified so far. Their inhibitory activities against picornaviruses and CoVs make these compounds broad-spectrum antiviral agents. With the escalating cost of drug discovery, development of an antiviral agent with broad-spectrum activities might help in overcoming financial hurdles. More compounds are being synthesized for lead optimization. Animal study needs to be further conducted for developing one of these potent inhibitors into an antiviral drug.

Acknowledgements

We appreciate Dr. Sung Soon Kim at Korea Centers for Disease Control and Prevention (KCDC) for providing MERS-CoV. This work was supported by Academia Sinica, Taiwan and the grants from KRICT (KK1603) and KCDC (2015-ER4808-00), Republic of Korea.

References

Akaji, K., Konno, H., Mitsui, H., Teruya, K., Shimamoto, Y., Hattori, Y., Ozaki, T., Kusunoki, M., Sanjoh, A., 2011. Structure-based design, synthesis, and evaluation of peptide-mimetic SARS 3CL protease inhibitors. J. Med. Chem. 54, 7962–7973.

Akaji, K., Konno, H., Onozuka, M., Makino, A., Saito, H., Nosaka, K., 2008. Evaluation of peptide-aldehyde inhibitors using R188I mutant of SARS 3CL protease as a proteolysis-resistant mutant. Bioorg. Med. Chem. 16, 9400–9408.

Anand, K., Ziebuhr, J., Wadhwani, P., Mesters, J.R., Hilgenfeld, R., 2003. Coronavirus main proteinase (3CL(pro)) structure: basis for design of anti-SARS drugs. Science 300, 1763–1767.

Barnard, D.L., Kumaki, Y., 2011. Recent developments in anti-severe acute respiratory syndrome coronavirus chemotherapy. Future Virol. 6, 615–631.

Chan, J.F., Chan, K.H., Choi, G.K., To, K.K., Tse, H., Cai, J.P., Yeung, M.L., Cheng, V.C., Chen, H., Che, X.Y., Lau, S.K., Woo, P.C., Yuen, K.Y., 2013. Differential cell line susceptibility to the emerging novel human betacoronavirus 2c EMC/2012: implications for disease pathogenesis and clinical manifestation. J. Infect. Dis. 207, 1743–1752.

de Wilde, A.H., Raj, V.S., Oudshoorn, D., Bestebroer, T.M., van Nieuwkoop, S., Limpens, R.W.A.L., Posthuma, C.C., van der Meer, Y., Bárcena, M., Haagmans, B.L., Snijder, E.J., van den Hoogen, B.G., 2013. MERS-coronavirus replication induces severe in vitro cytopathology and is strongly inhibited by cyclosporin A or interferon-α treatment. J. Gen. Virol. 94, 1749–1760.

Dyall, J., Coleman, C.M., Hart, B.J., Venkataraman, T., Holbrook, M.R., Kindrachuk, J., Johnson, R.F., Olinger Jr., G.G., Jahrling, P.B., Laidlaw, M., Johansen, L.M., Lear-Rooney, C.M., Glass, P.J., Hensley, L.E., Frieman, M.B., 2014. Repurposing of clinically developed drugs for treatment of Middle East respiratory syndrome coronavirus infection. Antimicrob. Agents Chemother. 58, 4885–4893.

Fan, K., Wei, P., Feng, Q., Chen, S., Huang, C., Ma, L., Lai, B., Pei, J., Liu, Y., Chen, J., Lai, L., 2004. Biosynthesis, purification, and substrate specificity of severe acute respiratory syndrome coronavirus 3C-like proteinase. J. Biol. Chem. 279, 1637–1642.

Ghosh, A.K., Xi, K., Ratia, K., Santarsiero, B.D., Fu, W., Harcourt, B.H., Rota, P.A., Baker, S.C., Johnson, M.E., Mesecar, A.D., 2005. Design and synthesis of peptidomimetic severe acute respiratory syndrome chymotrypsin-like protease inhibitors. J. Med. Chem. 48, 6767–6771.

Hilgenfeld, R., Peiris, M., 2013. From SARS to MERS: 10 years of research on highly pathogenic human coronaviruses. Antivir. Res. 100, 286–295.

Hsu, M.F., Kuo, C.J., Chang, K.T., Chang, H.C., Chou, C.C., Ko, T.P., Shr, H.L., Chang, G.G., Wang, A.H.J., Liang, P.H., 2005. Mechanism of the maturation process of SARS-CoV 3CL protease. J. Biol. Chem. 280, 31257–31266.

Ho, B.L., Cheng, S.C., Shi, L., Wang, T.Y., Ho, K.I., Chou, C.Y., 2015. Critical assessment of the important residues involved in the dimerization and catalysis of MERS coronavirus main protease. PLos One 10, e0144865.

Jetsadawisut, W., Nutho, B., Meeprasert, A., Rungrotmongkol, T., Kungwan, N., Wolschann, P., Hannongbua, S., 2016. Susceptibility of inhibitors against 3C protease of coxsackievirus A16 and enterovirus A71 causing hand, foot and mouth disease: a molecular dynamics study. Biophys. Chem. 219, 9–16.

Kilianski, A., Baker, S.C., 2014. Cell-based antiviral screening against coronaviruses: developing virus-specific and broad-spectrum inhibitors. Antivir. Res. 101, 105–112.

Kim, Y., Shivanna, V., Narayanan, S., Prior, A.M., Weerasekara, S., Hua, D.H., Kankanamalage, A.C., Groutas, W.C., Chang, K.O., 2015. Broad-spectrum inhibitors against 3C-like proteases of feline coronaviruses and feline calciviviruses. J. Virol. 89, 4942–4950.

Kumar, V., Jung, Y.S., Liang, P.H., 2013. Anti-SARS coronavirus agents: a patent review (2008-present). Expert Opin. Ther. Pat. 23, 1337–1348.

Kumar, V., Tan, K.P., Wang, Y.M., Lin, S.W., Liang, P.H., 2016. Identification, synthesis and evaluation of SARS-CoV and MERS-CoV 3C-like protease inhibitors. Bioorg. Med. Chem. 24, 3035–3042.

Kuo, C.J., Liang, P.H., 2015. Characterization and inhibition of the main protease of severe acute respiratory syndrome coronavirus. ChemBioEng Rev. 2, 118–132.

Kuo, C.J., Chi, Y.H., Hsu, J.T.A., Liang, P.H., 2004. Characterization of SARS main protease and inhibitor assay using a fluorogenic substrate. Biochem. Biophys. Res. Commun. 318, 862–867.

Kuo, C.J., Shie, J.J., Fang, J.M., Yen, G.R., Hsu, J.T.A., Liu, H.G., Tseng, S.N., Chang, S.C., Lee, C.Y., Shih, S.R., Liang, P.H., 2008. Design, synthesis, and evaluation of 3C protease inhibitors as anti-enterovirus 71 agents. Bioorg. Med. Chem. 16, 7388–7398.

Lee, C.C., Kuo, C.J., Ko, T.P., Hsu, M.F., Tsui, Y.C., Chang, S.C., Yang, S., Chen, S.J., Chen, H.C., Hsu, M.C., Shih, S.R., Liang, P.H., Wang, A.H., 2009. Structural basis of inhibition specificities of 3C and 3C-like proteases by zinc-coordinating and peptidomimetic compounds. J. Biol. Chem. 284, 7646–7655.

Matthews, D.A., Dragovich, P.S., Webber, S.E., Fuhrman, S.A., Patick, A.K., Zalman, L.S., Hendrickson, T.F., Love, R.A., Prins, T.J., Marakovits, J.T., Zhou, R., Tikhe, J., Ford, C.E., Meador, J.W., Ferre, R.A., Brown, E.L., Binford, S.L., Brothers, M.A., DeLisle, D.M., Worland, S.T., 1999. Structure-assisted design of mechanism-based irreversible inhibitors of human rhinovirus 3C protease with potent antiviral activity against multiple rhinovirus serotypes. Proc. Natl. Acad. Sci. U.S.A. 96, 11000–11007.

Needle, D., Lountos, G.T., Waugh, D.S., 2015. Structures of the Middle East respiratory syndrome coronavirus 3C-like protease reveal insights into substrate specificity. Acta Cryst. D71, 1102–1111.

Pillaiyar, T., Manickam, M., Namasivayam, V., Hayashi, Y., Jung, S.H., 2016. An overview of severe acute respiratory syndrome-coronavirus (SARS-CoV) 3CL protease inhibitors: peptidomimetics and small molecule chemotherapy. J. Med. Chem. 59, 6595–6628.

Ramajayam, R., Tan, K.P., Liang, P.H., 2011. Recent development of 3C and 3CL protease inhibitors for anti-coronavirus and anti-picornavirus drug discovery. Biochem. Soc. Trans. 39, 1371–1375.

Rota, P.A., Oberste, M.S., Monroe, S.S., Nix, W.A., Campagnoli, R., Icenogle, J.P., Penaranda, S., Bankamp, B., Maher, K., Chen, M.H., Tong, S., Tamin, A., Lowe, L., Frace, M., DeRisi, J.L., Chen, Q., Wang, D., Erdman, D.D., Peret, T.C., Burns, C., Ksiazek, T.G., Rollin, P.E., Sanchez, A., Liffick, S., Holloway, B., Limor, J., McCaustland, K., Olsen-Rasmussen, M., Fouchier, R., Gunther, S., Osterhaus, A.D., Drosten, C., Pallansch, M.A., Anderson, L.J., Bellini, W.J., 2003. Characterization of a novel coronavirus associated with severe acute respiratory syndrome. Science 300, 1394–1399.

Shie, J.J., Fang, J.M., Kuo, T.H., Kuo, C.J., Liang, P.H., Huang, H.J., Wu, Y.T., Jan, J.T., Cheng, Y.S., Wong, C.H., 2005. Inhibition of the severe acute respiratory syndrome 3CL protease by peptidomimetic α,β-unsaturated esters. Bioorg. Med. Chem. 13, 5240–5252.

St John, S.E., Tomar, S., Stauffer, S.R., Mesecar, A.D., 2015. Targeting zoonotic viruses: structure-based inhibition of the 3C-like protease from bat coronavirus HKU4-The likely reservoir host to the human coronavirus that causes Middle East Respiratory Syndrome (MERS). Bioorg. Med. Chem. 23, 6036–6048.

Thanigaimalai, P., Konno, S., Yamamoto, T., Koiwai, Y., Taguchi, A., Takayama, K., Yakushiji, F., Akaji, K., Chen, S.E., Naser-Tavakolian, A., Schon, A., Freire, E., Hayashi, Y., 2013. Development of potent dipeptide-type SARS-CoV 3CL protease inhibitors with novel P3 scaffolds: design, synthesis, biological evaluation, and docking studies. Eur. J. Med. Chem. 68, 372–384.

Thiel, V., Herold, J., Schelle, B., Siddell, S.G., 2001. Viral replicase gene products suffice for coronavirus discontinuous transcription. J. Virol. 75, 6676–6681.

Thiel, V., Ivanov, K.A., Putics, A., Hertzig, T., Schelle, B., Bayer, S., Weissbrich, B., Snijder, E.J., Rabenau, H., Doerr, H.W., Gorbalenya, A.E., Ziebuhr, J., 2003. Mechanisms and enzymes involved in SARS coronavirus genome expression. J. Gen. Virol. 84, 2305–2315.

Tomar, S., Johnston, M.L., St John, S.E., Osswald, H.L., Nyalapatla, P.R., Paul, L.N., Ghosh, A.K., Denison, M.R., Mesecar, A.D., 2015. Ligand-induced dimerization of Middle East respiratory syndrome (MERS) coronavirus nsp5 protease (3CLpro): implications for nsp5 regulation and the development of antivirals. J. Biol. Chem. 290, 19403–19422.

Tong, T.R., 2009. Therapies for coronaviruses. Part 2: inhibitors of intracellular life cycle. Expert Opin. Ther. Pat. 19, 415–431.

Tyrrell, D.A., Bynoe, M.L., 1965. Cultivation of a novel type of common-cold virus in organ cultures. Br. Med. J. 1, 1467–1470.

Webber, S.E., Okano, K., Little, T.L., Reich, S.H., Xin, Y., Fuhrman, S.A., Matthews, D.A., Love, R.A., Hendrickson, T.F., Patick, A.K., Meador 3rd, J.W., Ferre, R.A., Brown, E.L., Ford, C.E., Binford, S.L., Worland, S.T., 1998. Tripeptide aldehyde inhibitors of human rhinovirus 3C protease: design, synthesis, biological evaluation, and cocrystal structure solution of P1 glutamine isosteric replacements. J. Med. Chem. 42, 2786–2805.

Yang, H., Yang, M., Ding, Y., Liu, Y., Lou, Z., Zhou, Z., Sun, L., Mo, L., Ye, S., Pang, H., Gao, G.F., Anand, K., Bartlam, M., Hilgenfeld, R., Rao, Z., 2003. The crystal structures of severe acute respiratory syndrome virus main protease and its complex with an inhibitor. Proc. Natl. Acad. Sci. U. S. A. 100, 13190–13195.

Yang, S., Chen, S.J., Hsu, M.F., Wu, J.D., Tseng, C.T., Liu, Y.F., Chen, H.C., Kuo, C.W., Wu, C.S., Chang, L.W., Chen, W.C., Liao, S.Y., Chang, T.Y., Hung, H.H., Shr, H.L., Liu, C.Y., Huang, Y.A., Chang, L.Y., Hsu, J.C., Peters, C.J., Wang, A.H., Hsu, M.C., 2006. Synthesis, crystal structure, structure-activity relationships, and antiviral activity of a potent SARS coronavirus 3CL protease inhibitor. J. Med. Chem. 49, 4971–4980.

Zhao, Q., Weber, E., Yang, H., 2013. Recent developments on coronavirus main protease/3C like protease inhibitors. Recent Pat. Antiinfect. Drug Discov. 8, 150–156.

Zhu, L., George, S., Schmidt, M.F., Al-Gharabli, S.I., Rademann, J., Hilgenfeld, R., 2011. Peptide aldehyde inhibitors challenge the substrate specificity of the SARS-coronavirus main protease. Antivir. Res. 92, 204–212.